Electronic Supplementary Material (ESI) for Nanoscale.

SUPPORTING INFORMATION

Water-soluble silicon nanocrystals as NIR luminescent probes for time-gated biomedical imaging

Synthetic procedures

Synthesis of allyl functionalized SiNCs

Hydride terminated SiNCs were prepared through thermal disproportionation of Hydrogen Silsesquioxane (HSQ), according to literature procedure.[1] HSQ was prepared as follows: 22.5mL of toluene was added dropwise to a mixture composed by 6.16 mL of concentrated sulfuric acid (98%) and 3.11 mL of fuming sulfuric acid (20% SO_3) in a nitrogen purged and dry environment; the two phases were left stirring for 30 minutes under nitrogen atmosphere. Then $HSiCl_3$ (8 mL) in toluene (55 mL) was slowly added dropwise and the reaction was left stirring for an additional hour before the two phases were separated. The organic layer was washed with a saturated $CaCO_3$ solution. The solution was dried over $MgSO_4$, filtered and finally concentrated under vacuum. The product was collected as a white solid (2.2 g, yield 52%).

The produced HSQ powder was treated via thermally induced disproportionation under reducing atmosphere (93% N_2, 7% H_2) in a tube furnace at a heating rate of 16°C/min with a final temperature of 1100°C (for SiNCs of diameter ca. 4 nm), or 1200°C (for SiNCs of diameter ca. 5 nm) and kept at temperature one hour to finally obtain oxide-embedded silicon nanocrystals (SiNCs).

To remove the oxide matrix, 100 mg of oxide-embedded SiNCs were chemically etched with a 1:1:1 EtOH:H_2O:HF (48%) solution for 1.5 h (diameter ca. 3 nm), in the light, at room temperature under air atmosphere. The so-formed hydride-terminated SiNCs were extracted into three 5 mL portions of toluene and centrifuged. The sample was than rinsed with chloroform twice using the centrifuge (8000 rpm for 5 min, each cycle). The solid product was immediately transferred in a nitrogen purged glove-box and redispersed in oxygen-free anhydrous toluene.

Chlorosilane terminated SiNCs were prepared by adding 0.2 mL (1.5 mmol) of dimethylvinylchlorosilane (DMVSiCl) to the hydride-terminated SiNCs dispersion, in the presence of ca. 1.5 mg of 4-decylbenzene diazonium tetrafluoroborate (4-DDB).[2] The solution became transparent after few minutes and the reaction was left at room temperature overnight in order to completely passivate the surface of SiNCs. The solution is finally dried under vacuum to remove DMVSiCl in excess, then refilled with anhydrous toluene and kept under inert atmosphere.

Allyl terminated nanocrystals (*Scheme 1a*) were prepared through the Grignard nucleophilic addition to the chlorosilane passivated SiNCs.[3] In particular, 0.2 mL allyl magnesium bromide (1 M solution in diethyl ether) was added to the chlorosilane passivated SiNCs solution and left stirring overnight at room temperature. While the addition of the Grignard reagent results in a turbid solution for 5 nm SiNCs, no significant effect was observed on the 4 nm nanocrystals other than the quenching of the typical red emission under UV light excitation.

The samples are then extracted from the glove-box and acidified MeOH (0.5mL HCl in 20 mL of MeOH) is added to quench the residual Grignard and precipitate the nanocrystals. The dispersion is then precipitated and washed three times with MeOH, then dissolved again in toluene and stored in vials for further use. Proton NMR measurements of Si-allyl were conducted and proton signals from the double bonds appeared around 6 ppm confirming the functionalization.[2]

Synthesis of thiolated-PEG through esterification

Thiolated poly(ethylene glycol) (PEG-SH) was prepared as follows:[4] 4.4 g of poly(ethylene glycol), MW=2000 (PEG) was introduced in a three-necked flask equipped with a stirrer and a condenser. 50 mL of dry toluene were added to dissolve the PEG, then 261 µL (3 eq.) of 3-mercaptopropionic acid and few drops of fuming sulfuric acid were added. The flask was heated to reflux with an oil bath overnight, under nitrogen. The reaction was then checked with TLC and cooled to room

temperature. The reaction solution was concentrated under reduced atmosphere, then diethyl ether was added to precipitate the product. The product was transferred on a Gooch filter and washed three times with diethyl ether, dried under vacuum and collected as a white waxy solid 1.4 g (yield 32%). ^{1}H-NMR (400 MHz, $CDCl_3$) δ 4.26 – 4.23 CH_2O(m, 2H), 3.62 CH_2CH_2O(s, 200H), 2.75 CH_2SH (m, 2H), 2.66 CH_2CO (t, J = 7.3 Hz, 2H), 1.66 S*H* (t, J = 8.3 Hz, 1H).

Synthesis of PEG-Functionalised SiNCs by thiol-ene click reaction[5]

A batch of allyl functionalized SiNCs was dissolved in 10 mL of toluene, then 1g of thiolated PEG was added (*Scheme 1b*). After the PEG is completely dissolved, 15 mg of AIBN (azobisisobutyronitrile) was added to start the thiol-ene click reaction. The solution was purged with nitrogen for 20 min under ultrasonication to remove oxygen traces, then heated for 4h at 70°C. After cooling to room temperature, the suspension became slightly turbid. The sample was dried under vacuum, suspended in ethanol, then dried again and dissolved in distilled water. The ethanol addition is essential to maintain the colloidal stability of the resulting sample. A drastic change in polarity of the solvent from toluene to DW might induce aggregation of functionalized SiNCs. The excess PEG and the residual AIBN were removed by either dialysis (RC dialysis tube, Millipore, MW cut-off=14000) or high-pressure filtration (RC filter, Amicon® Stirred Cells, MW cut-off=14000). Finally, the sample is filtered over 0.22 µm RC syringe filter and stored at room temperature. Slight aggregation occurs over the course of several weeks in concentrated solution, but not in diluted solutions (10^{-4} – 10^{-5} M).

^{1}H-NMR spectrum of functionalized SiNCs shows new signals of methylene protons in proximity to the thiol-ether group, which is formed upon click reaction between allyl functionalized SiNCs and thiolated PEG. ^{1}H-NMR (400 MHz, $CDCl_3$) δ 4.17 (m, 2H), 3.59 (m, 186H), 2.83 (m, 2H), 2.66 (m, 2H), 2.56 (t, 2H), 1.63 (m, 2H).

^{1}H-NMR

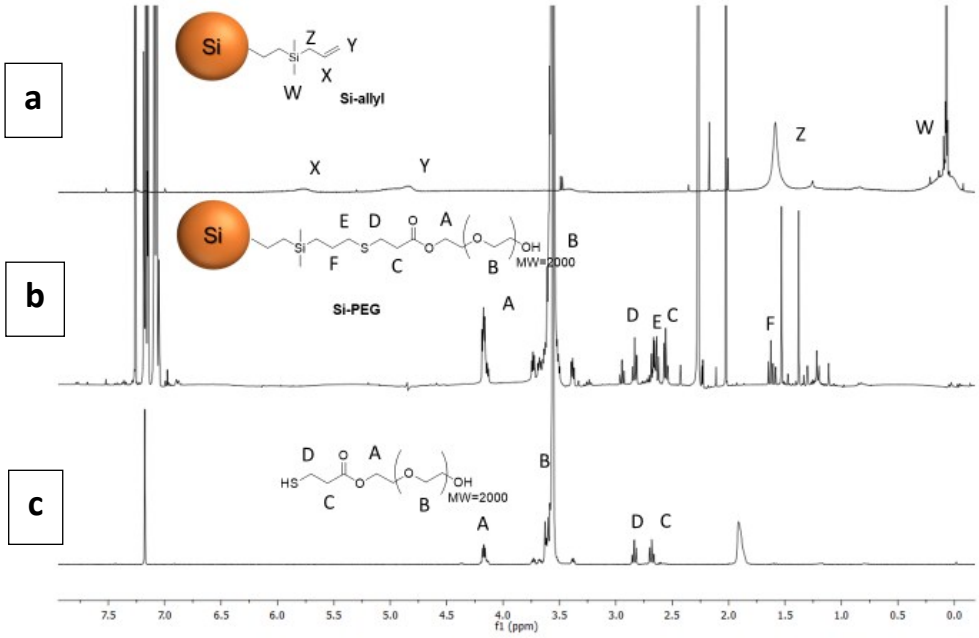

Figure S1. NMR spectra (400 MHz, $CDCl_3$) of (a) allyl functionalized silicon nanocrystals, (b) **Si-PEG** and (c) thiolated PEG

Figure S1 shows the NMR spectra of allyl functionalized SiNCs (*a*), **Si-PEG** (*b*) and the thiolated PEG(2000) (*c*). It is possible to observe that the signals related to the vinyl protons (indicated as X and Y) are present only in double bond functionalized SiNC, fading after the click reaction. Moreover, in **Si-PEG** spectrum, the signals of the ligand are preserved but broadened due to the molecules' low mobility at the nanoparicles' surface resulting in a longer relaxation time.[2,6]

TEM measurements.

High Resolution Transmission Electron Microscopy (HR-TEM) was carried out by a FEI Tecnai F20 instrument, equipped with a Schottky emitter and operated at 120 keV. EDX spectra were collected by focusing the beam on the region of interest and registered with an EDAX Phoenix spectrometer equipped with an ultra-thin window detector. The samples were prepared by drop casting on a CVD graphene coated TEM grid, in order to enhance the nanocrystals contrast due to the low thickness and atomic weight of the substrate.[7]

The TEM characterization of **Si-PEG** (d=5nm) is showing the presence of nanocrystals embedded in an amorphous matrix, which is consistent with the presence of the polymeric ligand. SiNCs diameter is (4.9 ± 1.2) nm, as displayed by the lognormal fitting of the size distribution displayed in Figure S2a. In addition, the EDS spectrum clearly shows an increasing amount of oxygen with respect to SiNCs passivated with simple dodecyl chains, sample available from previous work.[8]

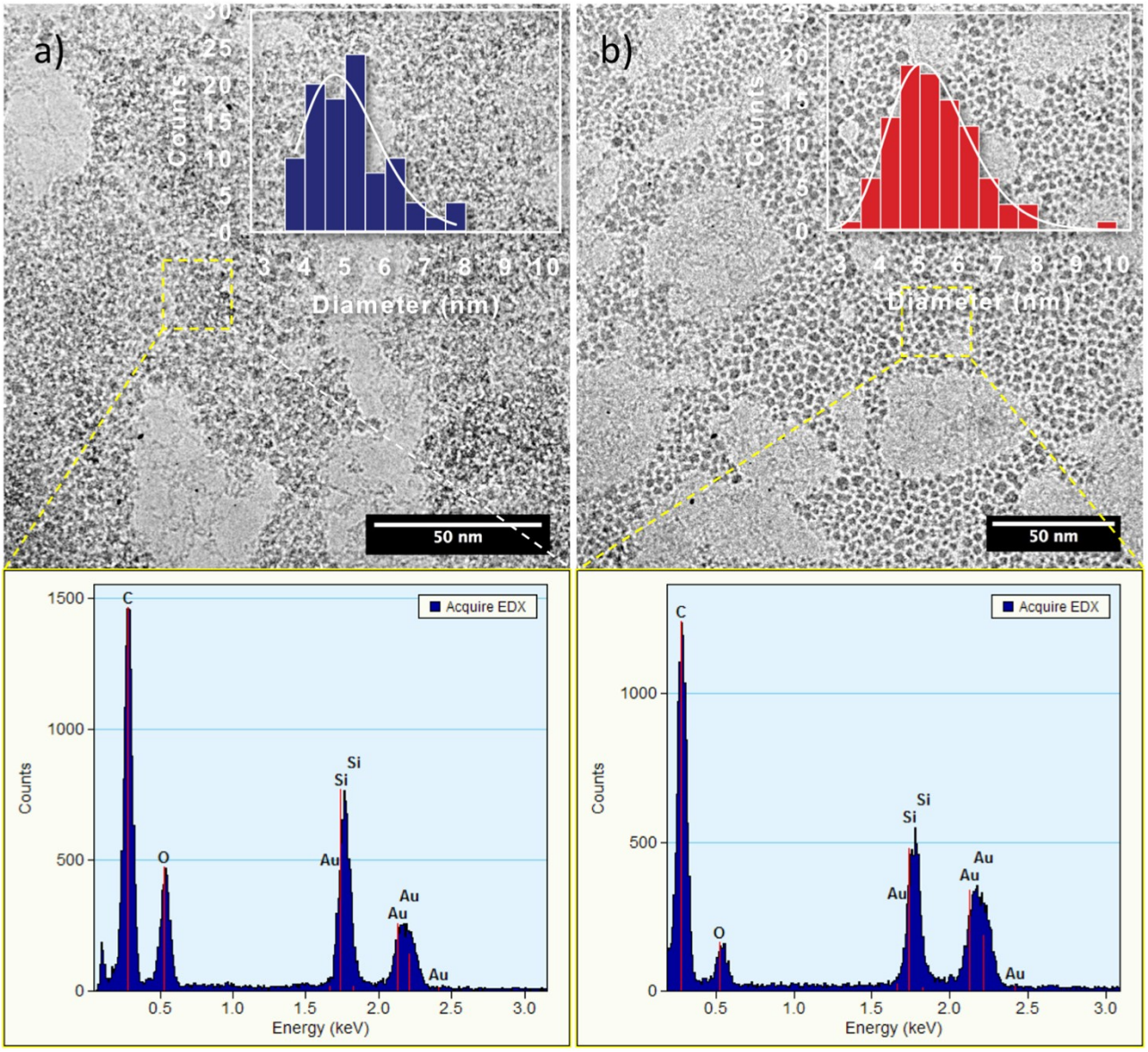

Figure S2. TEM micrograph (top) of **Si-PEG** (a) and SiNCs passivated with dodecyl chains (b), and corresponding EDS spectra (bottom) acquired on an area of the sample covered by SiNCs, as highlighted in the micrograph. Size distribution for both samples is displayed in the insets. The estimated nanocrystal diameter is: (4.9 ± 1.2) nm (a) and (5.1 ± 1.1) nm (b).

DLS analysis

The determination of the hydrodynamic diameter distributions of the nanocrystals was carried out by DLS measurements with a Malvern Nano ZS instrument with a 633 nm laser diode (*Figure S3*). Samples were housed in disposable polystyrene cuvettes of 1 cm optical path length. The calculated size was acquired on the basis of the volume occupied, and the main size class average was reported in the main text.

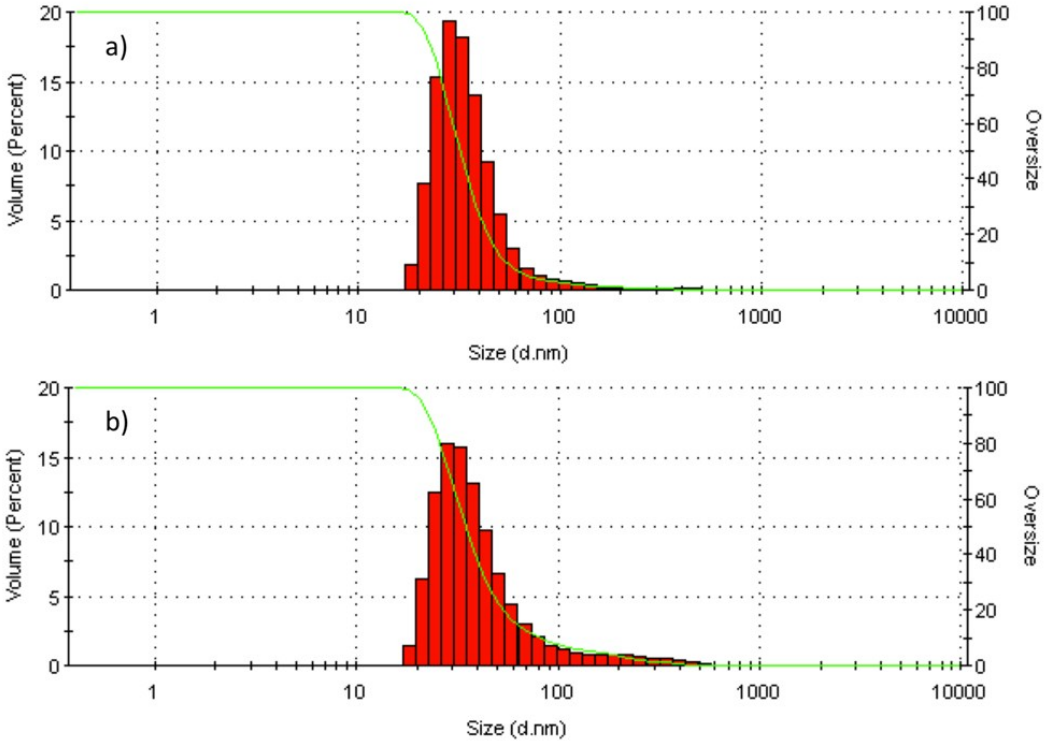

Figure S3. Dynamic light scattering analysis of a) 3 nm and b) 5 nm **Si-PEG** nanocrystals in water.

Photophysical measurements

Photophysical measurements were carried out in air-equilibrated distilled water at 298 K. UV-visible absorbance spectra were recorded with a Perkin Elmer λ650 spectrophotometer, using quartz cells

with 1.0 cm path length. Emission spectra were obtained with either a Perkin Elmer LS-50 spectrofluorometer, equipped with a Hamamatsu R928 phototube, or an Edinburgh FLS920 spectrofluorometer equipped with a Ge-detector for emission in the NIR spectral region. Correction of the emission spectra for detector sensitivity in the 700-1200 nm spectral region was performed by a calibrated lamp.[9] Emission quantum yields were measured following the method of Demas and Crosby[10] (standard used: $[Ru(bpy)_3]^{2+}$ in air-equilibrated aqueous solution Φ = 0.040[11] and HITCI (1,1',3,3,3',3'-hexamethyl-indotricarbocyanine iodide) in EtOH Φ = 0.30).[12] Emission intensity decay measurements in the range 10 µs to 1 s were performed on a homemade time-resolved phosphorimeter equipped with an Avalanche PhotoDiode C12703 with a peak sensitivity wavelength of 800 nm of the emitted light and a 365 nm pulsed LED as the excitation source. The estimated experimental errors are: 2 nm on the absorption and emission band maximum, 5% on the molar absorption coefficient and luminescence lifetime, and 10% on the luminescence quantum yield.

The size of the nanocrystals was determined by comparing the energy of the PL band maximum with the size-band gap correlation curve by following the method reported in[13].

Stability tests

Good stability is observed by diluting a small amount of 4 nm **Si-PEG** in distilled water. Lifetime values were recorded with a regular schedule by keeping the sample at room temperature (*Figure S4*).

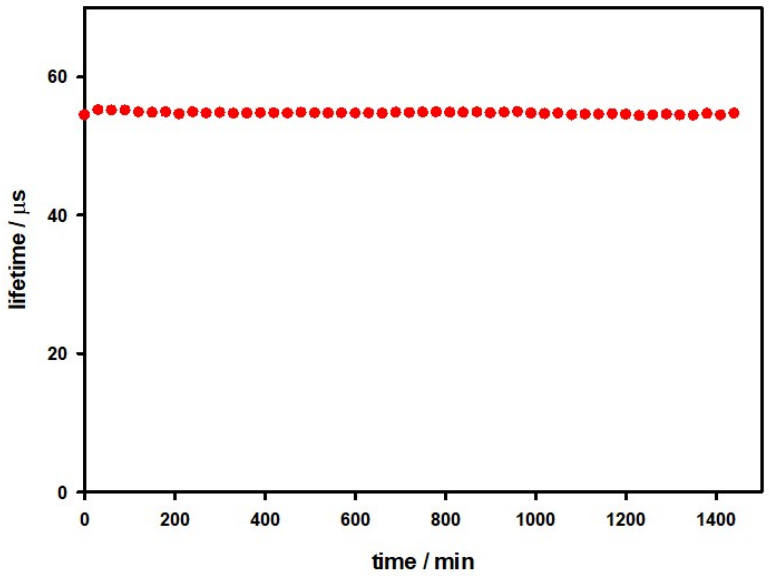

Figure S4. Stability test of 4 nm **Si-PEG** in distilled water at room temperature.

Quite good stability is observed by diluting a small amount of **Si-PEG** in human blood serum. Lifetime values were recorded with a regular schedule while heating the sample at 37°C for 4 hours (*Figure S5*). Luminescence lifetimes were also recorded as a function of pH with successive additions of KOH and HCl (*Figure S6*).

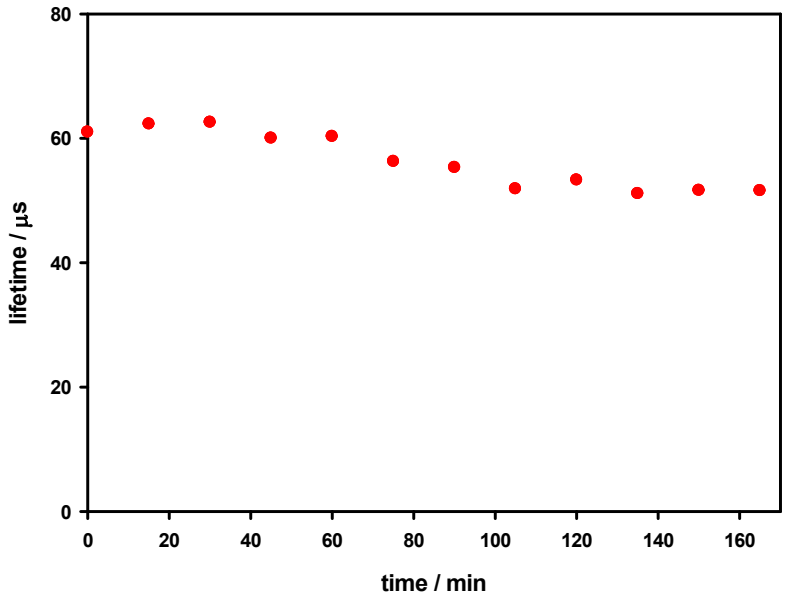

Figure S5. Stability test of **Si-PEG** in blood serum at 37°C.

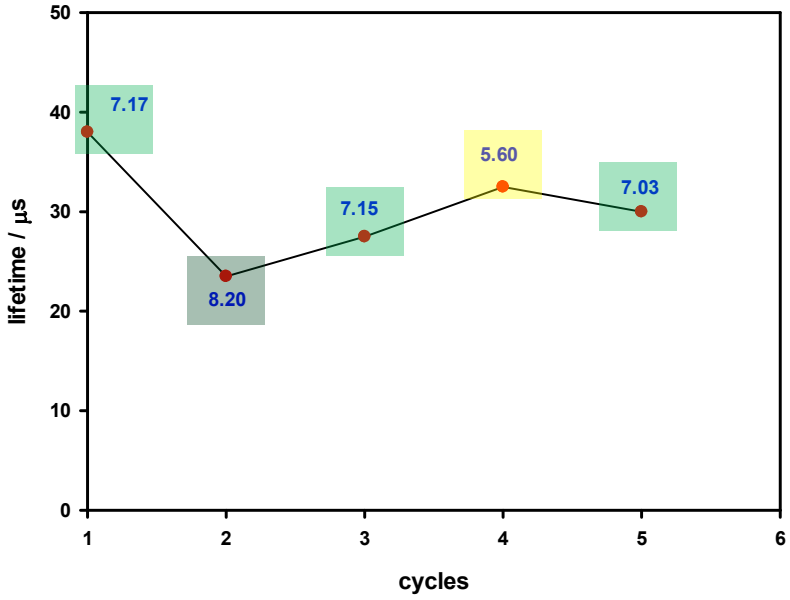

Figure S6. Luminescence lifetimes as a function of pH (values reported in blue) in successive additions of KOH and HCl to a 7.5 x 10^{-7} M solution of 4 nm **Si-PEG** in water. λ_{ex}=365nm; λ_{em} > 550nm.

Evaluation of oxygen influence on luminescent lifetimes

Dioxygen was removed from aqueous solutions of 4 nm **Si-PEG** using two enzymes, glucose oxydase and catalase[14]. These two enzymes in the presence of glucose and oxygen catalyze a reaction in which in the first step 1 eq of oxygen is consumed to produce hydrogen peroxide, and in the second step the peroxide regenerates 0.5 eq of oxygen and 0.5 eq of water. The net effect is that 0.5 eq. of oxygen is removed per catalytic cycle.

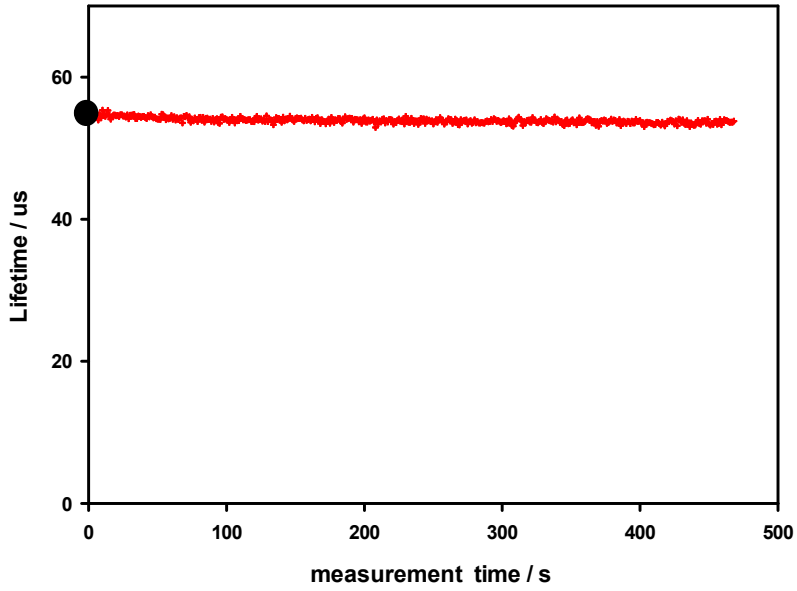

Figure S7. Luminescence lifetimes before (black dot) and after (red line) the addition of glucose oxidase and catalase.

In vivo animal studies

All animal procedures were approved by the Institutional Animal Care and Use Committee, and the studies here were carried out in compliance with these approved procedures. Briefly, 10^5 MDA-MB-231 cells were injected under the skin on the flank of a nude mouse (Charles River Laboratories, Wilmington, MA). Once tumors of approximately 100 mm^3 developed, these mice were then IV injected with 200 µL of 4 nm **Si-PEG** (1.5 µM) and were allowed to rest for 2, 4, 24, and 48 h prior to imaging. The animals were imaged both in vivo under anesthesia and then after sacrifice the organs were extracted for ex vivo imaging. The imaging was performed based on a custom fluorescence imaging system, which used a 457 nm Diode-pumped solid-state laser (DPSS laser, Laserglow Tech, Toronto ON Canada) for excitation and imaging with an ICCD camera (PI-MAX 4 1024i, Princeton Instruments, Acton MA USA) for optical signal collection. Figure S8 shows the profile of the laser intensity as a function of time. A 10 µs delay after a complete shutdown of the excitation source

was chosen for time-gated imaging. A function generator (Agilent 33120A, Agilent Technologies, Inc., Santa Clara, CA 95051, United States) was used to synchronize the ICCD camera and DPSS laser for time gating detection. A 1 kHz square wave with duty cycle of 20% was used to modulate the DPSS laser for time-gating mode, and 200 µs was accumulated on the ICCD camera with 100 µs delay after the falling edge. To increase the exposure time, 1000 frames were accumulated on the chip of the ICCD camera before each readout, so the total exposure time was 0.2 s. The gain was set to the maximum value for the ICCD camera to improve the detection sensitivity. A Sigma 70 mm f/2.8 DG ART macro lens was coupled with the ICCD camera, with a final field of view (FOV) of 10 cm x 10 cm. An 800 nm bandpass filter with full width at half maximum (FWHM) of 40 nm (Tharlab Inc. Newton, New Jersey, United States) was coupled between the lens and the ICCD camera to filter out the 457 nm laser when collecting the emission of SiNCs. For comparison between time-gated and continuous wave (CW) imaging, the latter was tested using the same laser and camera working with the same exposure time and accumulated number of frames, but in CW mode.

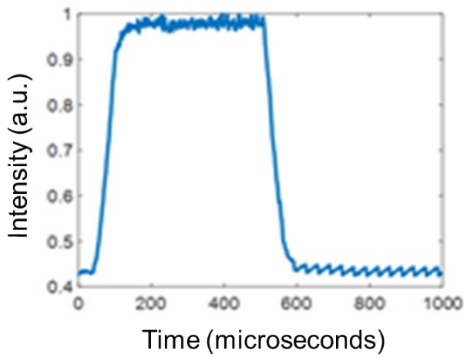

Figure S8. Intensity decay profile of the diode-pumped solid state laser

A measure of the localization of silicon nanocrystals in tumors and liver was conducted by evaluation of the ratio of the luminescence of the SiNCs in those tissues ex vivo as a function of time. Figure S9 shows that the maximum localization in tumors, due to EPR effect, occurred at 2 h post injection.

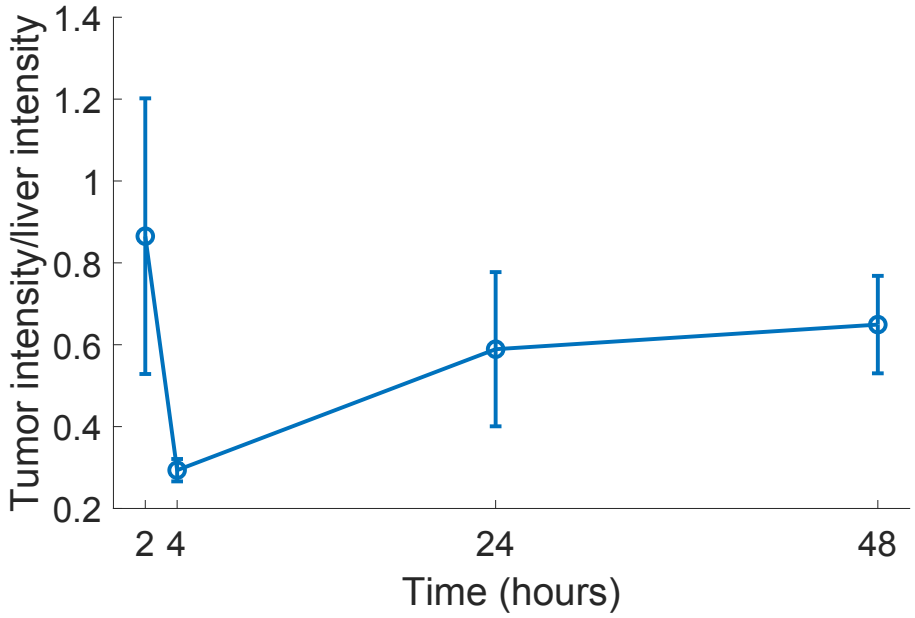

Figure S9. Ratio of the luminescence intensities of **Si-PEG** localized in tumours and liver measured ex-vivo as a function of time after in vivo injection. The intensity values and error bars are the average and standard deviation of luminescence intensities of all pixels in the tumor and liver area.

References

1. Hessel, C.M., Henderson, E.J., and Veinot, J.G.C. (2006). Hydrogen Silsesquioxane: A Molecular Precursor for Nanocrystalline Si−SiO2 Composites and Freestanding Hydride-Surface-Terminated Silicon Nanoparticles. Chem. Mater. *18*, 6139–6146.

2. Höhlein, I.M.D., Kehrle, J., Purkait, T.K., Veinot, J.G.C., and Rieger, B. (2015). Photoluminescent silicon nanocrystals with chlorosilane surfaces – synthesis and reactivity. Nanoscale *7*, 914–918.

3. Hessel, C. M.; Reid, D.; Panthani, M. G.; Rasch, M.R.., and Goodfellow, B. W.; Wei, J.; Fujii, H.; Akhavan, V.; Korgel, B.A. (2012). Synthesis of Ligand-Stabilized Silicon Nanocrystals with Size-Dependent Photoluminescence Spanning Visible to Near-Infrared Wavelengths. Chem. Mater *24*, 393−401.

4. Du, Y.J., and Brash, J.L. (2003). Synthesis and characterization of thiol-terminated poly(ethylene oxide) for chemisorption to gold surface. J. Appl. Polym. Sci. *90*, 594–607.

5. Ruizendaal, L., Pujari, S.P., Gevaerts, V., Paulusse, J.M.J., and Zuilhof, H. (2011). Biofunctional silicon nanoparticles by means of thiol-ene click chemistry. Chem. - An Asian J. *6*, 2776–2786.

6. Mazzaro, R., Gradone, A., Angeloni, S., Morselli, G., Cozzi, P.G., Romano, F., Vomiero, A., and Ceroni, P. (2019). Hybrid Silicon Nanocrystals for Color-Neutral and Transparent Luminescent Solar Concentrators. ACS Photonics *6*.

7. Panthani, M.M.G., Hessel, C.M.C., Reid, D., Casillas, G., José-Yacamán, M., and Korgel, B.A. (2012). Graphene-Supported High-Resolution TEM and STEM Imaging of Silicon Nanocrystals and their Capping Ligands. J. Phys. Chem. C *116*, 22463–22468.

8. Arrigo, A., Mazzaro, R., Romano, F., Bergamini, G., and Ceroni, P. (2016). Photoinduced Electron-Transfer Quenching of Luminescent Silicon Nanocrystals as a Way To Estimate the Position of the Conduction and Valence Bands by Marcus Theory. Chem. Mater. *28*, 6664–6671.

9. Ceroni, P. (2012). The Exploration of Supramolecular Systems and Nanostructures by Photochemical Techniques (Springer).

10. Crosby, G.A., and Demas, J.N. (1971). Measurement of photoluminescence quantum yields. Review. J. Phys. Chem. *75*, 991–1024.

11. Suzuki, K., Kobayashi, A., Kaneko, S., Takehira, K., Yoshihara, T., Ishida, H., Shiina, Y., Oishi, S., and Tobita, S. (2009). Reevaluation of absolute luminescence quantum yields of standard solutions using a spectrometer with an integrating sphere and a back-thinned CCD detector. Phys. Chem. Chem. Phys. *11*, 9850–9860.

12. Würth, C., Grabolle, M., Pauli, J., Spieles, M., and Resch-Genger, U. (2013). Relative and absolute determination of fluorescence quantum yields of transparent samples. Nat. Protoc. *8*, 1535–1550.

13. Mazzaro, R., Gradone, A., Angeloni, S., Morselli, G., Cozzi, P.G., Romano, F., Vomiero, A., and Ceroni, P. (2019). Hybrid Silicon Nanocrystals for Color-Neutral and Transparent Luminescent Solar Concentrators. ACS Photonics *6*, 2303–2311.

14. Vanderkooi, J.M., Maniara, G., Green, T.J., and Wilson, D.F. (1987). An optical method for measurement of dioxygen concentration based upon quenching of phosphorescence. J. Biol. Chem. *262*, 5476–5482.